JAAS

Journal of Analytical Atomic Spectrometry

www.rsc.org/jaas

Volume 25 | Number 3 | March 2010 | Pages 217–436

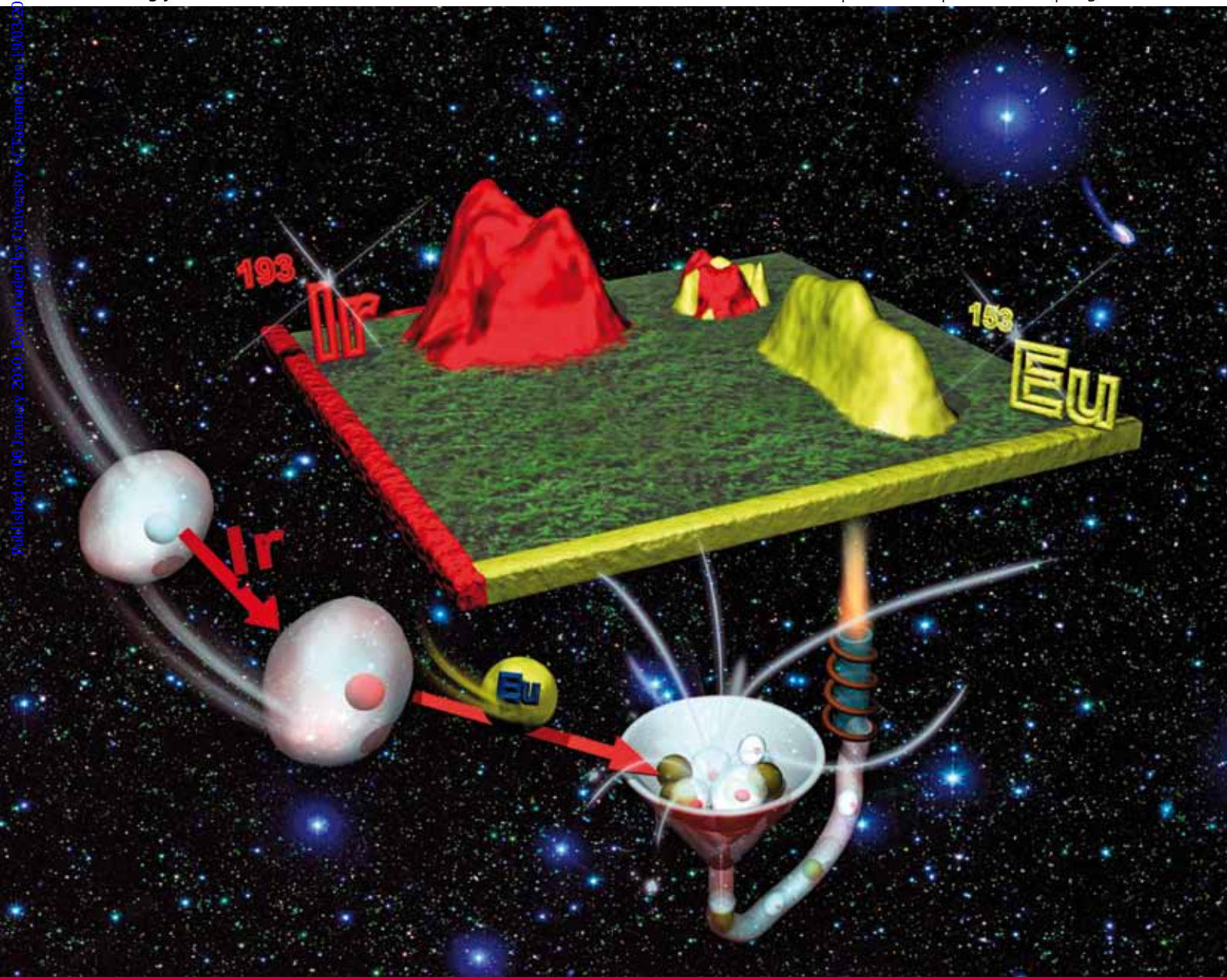

Themed Issue: Young Analytical Scientists

ISSN 0267-9477

RSC Publishing

HOT PAPER
Abdelrahman *et al.*
Metal-containing polystyrene beads as standards for mass cytometry

HOT PAPER
Chan and Hieftje
Algorithm to determine matrix-effect crossover points for overcoming interferences in inductively coupled plasma-atomic emission spectrometry

0267-9477(2010)25:3;1-F

Metal-containing polystyrene beads as standards for mass cytometry†‡

Ahmed I. Abdelrahman, Olga Ornatsky, Dmitry Bandura, Vladimir Baranov,* Robert Kinach, Sheng Dai, Stuart C. Thickett, Scott Tanner and Mitchell A. Winnik*

Received 20th October 2009, Accepted 15th December 2009
First published as an Advance Article on the web 6th January 2010
DOI: 10.1039/b921770c

We examine the suitability of metal-containing polystyrene beads for the calibration of a mass cytometer instrument, a single particle analyser based on an inductively coupled plasma ion source and a time of flight mass spectrometer. These metal-containing beads are also verified for their use as internal standards for this instrument. These beads were synthesized by multiple-stage dispersion polymerization with acrylic acid as a comonomer. Acrylic acid acts as a ligand to anchor the metal ions within the interior of the beads. Mass cytometry enabled the bead-by-bead measurement of the metal-content and determination of the metal-content distribution. Beads synthesized by dispersion polymerization that involved three stages were shown to have narrower bead-to-bead variation in their lanthanide content than beads synthesized by 2-stage dispersion polymerization. The beads exhibited insignificant release of their lanthanide content to aqueous solutions of different pHs over a period of six months. When mixed with KG1a or U937 cell lines, metal-containing polymer beads were shown not to affect the mass cytometry response to the metal content of element-tagged antibodies specifically attached to these cells.

Introduction

Immunophenotyping is a cellular analysis methodology for the identification of biomarkers using fluorescently conjugated affinity reagents. This is one of the key advances in medicinal research, which employs antibodies that are reactive against cell antigens to distinguish specific subsets within a heterogeneous mixture of cells. In such an assay, the quantification of a subset of interest can be readily accomplished on a cellular level by the use of a *flow cytometer*. To detect the presence of a cell-bound monoclonal antibody by flow cytometry, the antibody must be coupled either directly or indirectly to a fluorescent tag (*e.g.* fluorescent dyes or quantum dots).[1–8] The differentiation of fluorophores can be achieved by detection of their different emission spectra. Quantitation of these fluorescence signals provides the determination of the amount of fluorophore bound to a particular cell. With the use of appropriate standards, the amount of detected fluorophore can be used to estimate the number of antigens targeted by the fluorescence-tagged antibody.

In many cases, fluorescence standards are calibration beads which contain fluorophore(s) with sharp signals that can be used to generate a calibration curve.[9–13] Much less frequently, these beads can be mixed with the sample of interest for use as an internal standard.[14,15] The main limitation of fluorescence-based immunoassays, however, is the low variability in both the type and number of different fluorophores with emission intensities that can be adequately resolved to allow for simultaneous detection. In addition to this limitation, the broadness of emission spectra and the different excitation wavelengths of different fluorophores further complicate such measurements. Some of these problems can be mitigated by using quantum dots with very narrow size distributions, which give significantly narrower emission bands.[16] However, the limited linear dynamic range of fluorescence-based assays makes quantitative analysis using flow cytometry challenging. This challenge is particularly apparent during the analysis of samples that consist of analytes that differ in concentration by more than an order of magnitude.

A much larger amount of information can be obtained using different metal atoms or isotopes as labels, coupled with their detection by atomic mass spectrometry.[17,18] Metal-encoded beads coupled with mass cytometry based on inductively coupled plasma mass spectrometry detection opens the door to multiplexed analyses that can differentiate over an order of magnitude more unique labels than what is possible with assays based upon luminescence detection.[19–21] Expanding on the concept of the fluorochrome bead assays of conventional flow cytometry, we have incorporated different metals (or individual isotopes) into polymer beads at different levels of concentration,[22] with bead-by-bead detection and readout based upon mass cytometry instrumentation.[23–26] The quantification of data possible *via* mass cytometry provides an absolute determination of the number of ions in the sample, rather than the relative or semi-quantitative processes used in conventional flow cytometers. It is worth noting that the behaviour of different elements in an Ar plasma torch depends on their physical properties, such as atomic mass and ionization efficiency but these variations are constant for

Department of Chemistry, University of Toronto, 80 St George Street, Toronto, ON, M5S3H6, Canada. E-mail: mwinnik@chem.utoronto.ca; vladimir.baranov@utoronto.ca

† This article is part of a themed issue devoted to highlighting the work of outstanding young analytical scientists (YAS) working in the area of analytical atomic spectrometry. This 3rd YAS issue has been guest edited by Professor Spiros Pergantis.

‡ Electronic supplementary information (ESI) available: Microwave digestion protocol, SEM image of beads of samples AA086-Tm, mass cytometry signal intensity distribution for ^{159}Tb from samples AA083-Tb. The mass cytometry signal intensity distribution for ^{159}Tb and ^{169}Tm. See DOI: 10.1039/b921770c

a robust plasma. In order to effectively correct for temporal variations in signal intensity (usually caused by the instrument tuning and drift), the use of standard calibration beads is important. The calibration will account for the variations between different mass cytometer instruments and for the slight signal drift during mass spectra acquisition. Internal standard beads which are added directly to the samples in known quantity should have known concentrations of metal(s) with atomic masses and ionization efficiencies close to those of the metal tag.[27] Also, the efficiency of the sample introduction system can be assessed by the number of registered bead events per acquisition time. This number can be used to estimate the number of cells in the sample if the efficiency of the sample introduction system is less than perfect.

In this article, we describe the synthesis and the utilization of metal-containing polymer beads as *standard beads* for mass cytometry instrument calibration and as *internal standards* for cell analysis. We use synthetic methods similar to those that we have described in ref. 22 for the synthesis of lanthanide-encoded *classifier* beads for mass cytometry-based immunoassays. The focus here is on exploring the upper detection limit of mass cytometry, as well as optimizing the lanthanide content of the beads to fall in the detection range of the instrument. In addition, we show proof of principle experiments in which beads are mixed with different cell lines and subjected to mass cytometry.

Experimental

Materials

Styrene (Aldrich), acrylic acid (AA, Aldrich), absolute ethanol, polyvinylpyrrolidone (PVP) (Aldrich, PVP55, M = 55,000), Triton-X305 (TX305, 70% solution in water, Aldrich), 2,2′-azobis(2-methylbutyronitrile) (AMBN, Dupont USA), ethylene glycol dimethacrylate (EGDMA, Aldrich), lanthanum(III) chloride hydrate ($LaCl_3$, Fluka), thulium(III) chloride hexahydrate ($TmCl_3$, Aldrich), europium(III) chloride hexahydrate ($EuCl_3$, Aldrich), terbium(III) chloride hexahydrate ($TbCl_3$, Aldrich), holmium(III) chloride hexahydrate ($HoCl_3$, Aldrich), and praseodymium(III) chloride hexahydrate ($PrCl_3$, Aldrich) were used without further purification. Water was purified through a MilliQ purification system. High purity HCl and HNO_3 for ICP-MS analysis were purchased from Seastar Chemical Inc. Phosphate-buffered saline with calcium and magnesium (PBS; 150 mM NaCl, 1.2 mM Ca^{2+}, 0.8 mM Mg^{2+}, 20 mM sodium phosphate, pH 7.4), 37% formaldehyde (Sigma), Ir (iridium) diluted from stock 1000 μg mL^{-1} solutions (PE) to 1 ng mL^{-1} in 3.3–3.6% HCl. All solutions for bioassays were prepared in deionised water (Elix/Gradient water purification system, Millipore).

Antibodies. Primary mouse monoclonal antibodies (mAb) *anti*-CD34 mAb, 0.25 mg mL^{-1} (BD Biosciences), were used at 1 : 100 dilution; Antibodies were labeled with the prototype MAXPAR reagents (DVS Sciences Inc., Richmond Hill, Ontario, Canada; www.DVSsciences.com), based on metal-labeled polymer tags described in detail by Lou *et al.*[27]

Cell lines. Human monocyte cell line KG1a, a model human acute myelogenous leukemia cell line, with high CD34 antigen expression (approximately 100 000 copies per cell), as well as U937 human leukemic monocyte lymphoma cell line (that does not express CD34), were obtained from the American Type Culture Collection (Manassas, VA). Cells were propagated in MEM synthetic media, supplemented with 10% FBS (HyClone) and 2 mM L-glutamine (Invitrogen), in a humidified incubator at 37 °C and 5% CO_2. Cells were split every 3–4 days, and viability was checked with trypan blue (>90% viable).

Metallointercalator. The Ir-containing metallointercalator (pentamethylcyclopentadienyl)-Ir(III)-dipyridophenazine, Ir-intercalator, is the sample described in Ref. 21. This Ir-intercalator is indefinitely stable in the solid state and in aqueous solution. This Ir-intercalator complex was found to have an equilibrium constant K_b of 2.6×10^6 M^{-1} for binding to double-stranded DNA. It is used here to stain the cell DNA.

Two and three-stage dispersion polymerizations

The standard recipe for the two-stage dispersion polymerization (2-DisP) of styrene with AA in ethanol is listed in Table 1. The procedure used is similar to the one described in Ref. 22, in which the PS-co-PAA beads were obtained after 24 h reaction under ethanol-saturated nitrogen in the presence of PVP55 as a dispersant. In these reactions, AA and the lanthanide chloride salt were added in the second stage, one hour after initiating the polymerization. Gravimetric measurements showed that conversions of approximately 95–99% were obtained.

In the three-stage dispersion polymerization reaction (3-DisP, sample AA120-Eu), additional AA and a small amount of crosslinking agent, EGDMA, in 10 ml ethanol were heated to 70 °C and added to the reaction after the polymerization reaction had run for 16 h (*ca.* 80% styrene conversion). More details about the 2-DisP and 3-DisP reactions are given in Ref. 22.

Characterization of particle sizes and size distributions

The bead diameters and diameter distributions were determined from images obtained with a Hitachi S-5200 FE-scanning electron microscope (SEM). The samples for SEM imaging were prepared by placing a drop of a diluted suspension on a Formvar/carbon coated-300 mesh copper grid to obtain a single layer of beads. There was no need to purify the beads by

Table 1 Recipes for the dispersion polymerization of styrene with PVP55 and acrylic acid in ethanol

	Two-stage reaction		Three-stage reaction		
Materials (g added)	1st stage	2nd stage	1st stage	2nd stage	3rd stage
Styrene	6.25	—	6.25	—	—
PVP55 [a]	1.0	—	1.0	—	—
TX305 [b]	0.35	—	0.35	—	—
AMBN [c]	0.25	—	0.25	—	—
Ethanol	18.75	18.75	18.75	10.0	10.0
Acrylic acid	—	0.125	—	0.125	0.125
$LnCl_3$	—	[d]	—	[d]	—
EGDMA	—	—	—	—	0.063

[a] polyvinylpyrrolidone, M ≈ 55 kDa. [b] Triton X-305. [c] azomethylbutyronitrile. [d] AA070-Tm: 6.3 mg $TmCl_3.6H_20$; AA086-Tm: 0.63 mg $TmCl_3.6H_20$, and AA120-Eu: 0.63 mg $EuCl_3.6H_20$.

centrifugation and resuspension in alcohol to obtain clear images. A particle-size histogram was constructed from measurements of at least 200 individual beads for each sample.

Microwave digestion

To examine the metal content of the beads by conventional ICP-MS, the beads were first microwave-digested in concentrated HNO_3. According to a published procedure,[28] 15 mg of freeze dried and finely ground bead sample was wet-oxidised with 8 mL of the nitric acid. The digestion protocol is shown in Table S1, ESI.‡ High-pressure 50-mL quartz vessels were used, and these were heated in a Perkin-Elmer/Paar Physica multiwave high-pressure digestion system with infrared temperature control and hydraulic pressure control. This instrument has a maximum microwave power of 1000 W/2420 kHz, the maximum operating pressure 7400 kPa (74 bar). A vessel that contains only HNO_3 was included in the digestions as a blank.

Lanthanide ion content and release behavior

The lanthanide ion content of each sample was measured by mass cytometry. Data reported here refer to analysis of 10 000 to 20 000 individual beads.

The lanthanide ion release behaviour of sample AA120-Eu was examined by traditional ICP-MS. The lanthanide-containing beads were first washed by 3 centrifugation-resuspension steps using deionised water and then resuspended in three different buffer solutions (solids content 0.5 wt %), namely 10 mM ammonium acetate (pH 7.0), 50 mM sodium acetate (pH 3.0) and sodium carbonate/bicarbonate 200 mM (pH 10.6). Aliquots were taken at regular time intervals over a six-month period and sedimented by centrifugation at 5000 rpm. The supernatant was then subjected to ICP-MS analysis.

Instrumentation

Mass cytometry. Mass cytometry experiments were carried out using a CyTOF™ instrument from DVS Sciences (Toronto ON Canada, www.dvssciences.com). The instrument is commercially available and has been described in detail elsewhere.[23] Briefly, this instrument employs an inductively coupled plasma ion source and a time-of-flight mass analyzer operating at 76.8 kHz spectrum generation and recording frequency. The instrument provides the capability of collecting multiple spectra from each particle-induced transient ion cloud, typically of 200–300 microseconds duration, with a user selectable mass resolution ranging from 300 to 900 (f.w.h.m.). The transients can be resolved and characterized individually at a peak frequency of 1100 particles per second.

Analog-to-digital conversion (ADC) data from the PDA1000 digitizer (Signatec, Inc., Newport Beach, CA, USA) was used in two ways: to provide ion counting mode for low intensity signals (counting mode) and analog data collected for high intensity signals (analog mode). In the counting mode, distinct peaks from single ions within each m/z time-of-flight interval are detected separately in each single push-out spectrum. The detector was calibrated employing the best linear fit correlation between the analog and pseudo-counting signals.

The figures of merit of the instrument are measured under standard ICP operating conditions of a robust plasma (defined as a ratio of $CeO^+/Ce^+ < 3\%$). At mass resolution (full width at half maximum) for $m/z = 159$, $M/\Delta M > 900$, the sensitivity with standard sample aspiration is typically 1.4×10^8 ion counts per second per mg L^{-1} of Tb, and the abundance sensitivity is $6 \times 10^{-4} - 1.4 \times 10^{-3}$ (trailing and leading masses, respectively). The mass range (variable, but fixed at $m/z = 125 - 215$ for this work) and the abundance sensitivity are sufficient for elemental encoding with up to 60 distinct isotopes. More details about this instrument can be found in Ref. 22–24.

ICP-MS. Sample analyses by ICP-MS employed an ELAN 9000 instrument (Perkin-Elmer SCIEX). Typical operating conditions of the instrument are based on stable Ar plasma optimized to provide less than a 3% CeO^+/Ce^+ ratio in a 1 ppb standard multielement solution diluted in a 1 : 10 dilution of concentrated (33 – 36 wt %) HCl, *i.e.* 3.3 – 3.6% HCl. This requirement was achieved by applying 1400 W forward plasma power, 17 L min^{-1} Ar plasma gas flow, 1.2 L min^{-1} auxiliary Ar flow, and 0.95 L min^{-1} (Perkin-Elmer cross flow) nebulizer Ar flow. Under these operating conditions, the typical sensitivity is 4×10^4 cps for 1 ppb Ir standard solution in 3.3 – 3.6% HCl. The detection limits for lanthanide elements were less than 1 ppt. The sample uptake rate was adjusted depending on the particular experiment and sample size, typically 100 μL min^{-1}. Experiments were performed using an autosampler (Perkin-Elmer AS 93) modified for operation with Eppendorf 1.5 mL tubes. Sample sizes varied from 150 to 300 μL. Standards were prepared from 1000 μg mL^{-1} PE Pure Single-Element Standard solutions (Perkin-Elmer, Shelton, CT) by sequential dilution with high-purity deionised water (DIW) produced using an Elix/Gradient (Millipore, Bedford, MA) water purification system.

Results and discussion

When we began our project to synthesize reagents for bioassays based upon ICP-MS detection, members of the lanthanide (Ln) family were selected to be the metal tags.[27,29] This family of elements was chosen for their low natural abundance, the large number of stable resolvable isotopes (54 in total) and their similar chemistry.[30] In our initial experiments, we designed and synthesized metal-chelating polymers for lanthanides to attach to monoclonal antibodies. These metal polymer-tagged antibodies were then used in conjunction with ICP-MS bioassays for phenotyping human leukemia cells.[29] In later experiments, we designed and synthesized lanthanide-containing polymer nanoparticles and microparticles. The nanoparticles were used for cell labeling (*via* non-specific endocytosis), whereas the microparticles are intended to be used in bead-array type assays.[22]

For metal-containing beads to be used as internal standards or calibration standards in mass cytometry, four major requirements must be met. First, the beads must be large enough to be easily injected into the mass cytometer on a bead-by-bead basis, but small enough to guarantee complete burning and ionization of the beads in the ICP torch. Polystyrene beads with diameters in the range of 0.8 to 3.0 μm satisfy these requirements. Beads of this size are also convenient to manipulate in terms of washing and redispersing. We characterize particle size in terms of the

mean particle diameter (d) obtained from the analysis of SEM images. These metal-containing beads should also have a very narrow size distribution. We characterize the size distribution in terms of coefficient of variation of the particle diameter (CV_d).

$$CV_d = \frac{1}{D_{av}}\sqrt{\frac{1}{n-1}\sum_{i=1}^{n}(D_i - D_{av})^2} \quad (1)$$

where D_{av} is the number average diameter of all particles, D_i is the diameter of the i'th particle, and n is the total number of particles counted in the analysis

Second, the metal-containing beads must have a very small bead-to-bead variation in lanthanide content. We characterize the lanthanide content by determining the average number of Ln atoms per bead. Ln variation from bead-to-bead will be evaluated by the magnitude of the Ln coefficient of variation (CV_{Ln}), which is obtained from the mass cytometry measurement. This value is defined by an expression analogous to that in eqn (1). We expect that $CV_{Ln} \geq CV_V$, the coefficient of variation of the particle volume. At this moment we do not have a clear way to differentiate between measurement and content contributions to CV_{Ln}.

Third, each bead must have a lanthanide-content close to the middle of the detection range of the mass cytometer. We will show how we define this concentration and how we designed the polymer bead synthesis to meet this requirement. Finally, metal-containing beads to be used as calibration standards should retain their lanthanide content in fluid media during prolonged storage as well as during experimental assays. This will be gauged by determining Ln release behaviour from the particle interior as a function of time.

Bead synthesis and metal incorporation

For the synthesis of lanthanide-containing polymer beads, we employed the same technique described in our recent publication,[22] for the synthesis of monodispersed PS-*co*-PAA beads. The synthesis is based on the dispersion polymerization of styrene in ethanol in the presence of polyvinylpyrrolidone (PVP).[31] In this synthesis strategy, the addition of the acrylic acid is delayed until the particle nucleation step is complete (a few percent monomer conversion). We refer to this method as "two-stage" dispersion polymerization (denoted 2-DisP). Thus in our design, we initiate dispersion polymerization of styrene in ethanol, and after approximately 10% monomer conversion, add known amounts of $LnCl_3$ in ethanol in the presence of an excess of acrylic acid (AA) that serves as a ligand for Ln^{3+}. The carboxylate group of AA is known to interact strongly with lanthanide ions. The reagents employed in these 2-DisP reactions and the amounts of $LnCl_3$ salt used are presented in Table 1. The characteristics of the particle samples synthesized are collected in Table 2. The reactions were clean, and yielded particles in 90–95% gravimetric yield, with no coagulum.

We were first interested in testing the range of lanthanide ion concentrations that can be studied by mass cytometry. The current research prototype mass cytometry instrument[23,24] provides an ion transmission efficiency of $T \approx 5 \times 10^{-5}$, which yields a sensitivity on the order of 200 counts per second per part per trillion. To see if high loadings of metal ions would saturate the detector, we designed a synthesis that would yield beads

Table 2 Particle size, size distribution, and the variation of Tm and Eu content for some PS-PAA beads synthesized in the presence of $LnCl_3 \cdot 6H_2O$

Sample	$d \pm \sigma_d$[a]/μm	CV_d%[a]	Ln loading[b]	Ln measured[c]	CV_{Ln}%[d]
AA070-Tm	2.1 ± 0.052	2.5	1.00	8.0×10^7	25
AA086-Tm	1.9 ± 0.066	3.4	0.10	1.1×10^7	37
AA120-Eu[e]	2.2 ± 0.035	1.6	0.10	1.2×10^7	14

[a] d = mean diameter; σ_d = one standard deviation; CV_d = coefficient of variation of the diameter. [b] Ln loading: wt %/styrene of $LnCl_3 \cdot 6H_2O$ based upon styrene used in the particle synthesis, see Table 1. [c] The number of Tm and Eu atoms per bead from the mass cytometry intensity and calculated by eqn (2). [d] CV of ^{169}Tm and ^{153}Eu intensity measured by mass cytometry. [e] Synthesized by 3-stage dispersion polymerization.

containing *ca.* 10^8 copies of an individual isotope. We selected ^{169}Tm as a mono-isotopic element, and synthesized the AA070-Tm sample, described in Table 1, in which 1.0 wt%/sty $TmCl_3$ and 2.0 wt%/sty AA were added in the second stage. The incorporation efficiency of the lanthanide ions is the percentage of lanthanide ions added in the reaction that were incorporated into the beads. According to the high lanthanide ion incorporation efficiency obtained in the syntheses described in Ref. 22, we based our calculations on the assumption of complete encapsulation of Ln ions into the polymer beads. Fig. 1 shows a scanning electron microscope (SEM) image of sample AA070-Tm. The sample has mean a diameter $d = 2.1$ μm, with a narrow size distribution ($CV_d = 2.5\%$).

To examine the metal ion (^{169}Tm) content of sample AA070-Tm, this bead dispersion was washed by three cycles of centrifugation and resuspension in water. The resultant slurry (*ca.* 10^6 beads/mL) was nebulised into the mass cytometer sample introduction system, which in turn delivered beads individually but stochastically into the inductively coupled plasma torch. The high temperature of the plasma was sufficient to vaporize, atomize and then ionize the beads and the Tm ions embedded in them. The ion stream was then introduced into the time-of-flight mass analyzer. The transient signals corresponding to each bead ionization event were recorded by the detector and stored.

The histogram representation of the frequency distribution of the integrated ion intensity over the transient signal for

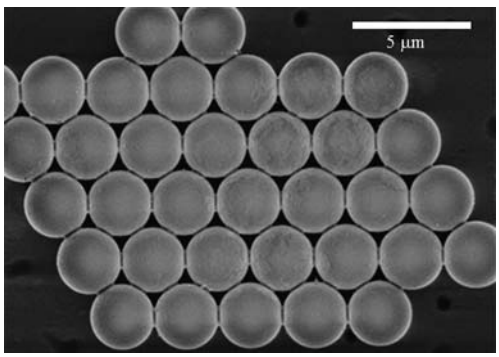

Fig. 1 SEM image of PS bead sample AA070-Tm synthesized in the presence of 1% $TmCl_3$ added in the second stage with AA: 2 wt %/styrene ($d = 2.1$ μm, $CV_d = 2.5\%$).

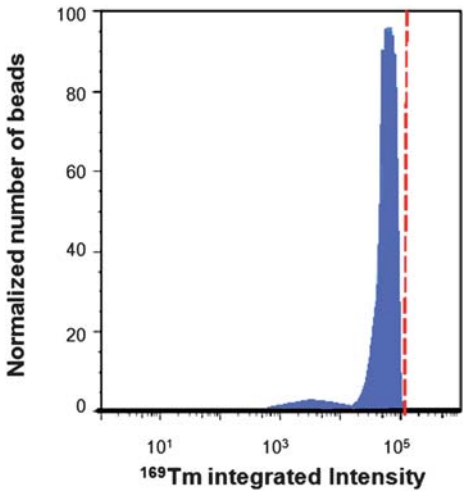

Fig. 2 Distribution of mass cytometry intensity signal for a population of PS beads (AA070-Tm) prepared by 2-DisP in presence of $TmCl_3$ (1.0 wt%/styrene) and AA (2.0 wt%/styrene). The dashed-line indicates the sharp cutoff at *ca.* 10^5 ^{169}Tm signal intensity that this is likely due to detector saturation.

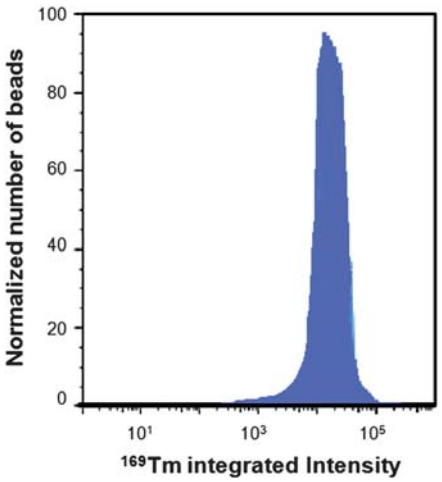

Fig. 3 Distribution of mass cytometry intensity signal for a population of PS beads (AA086-Tm) prepared by 2-DisP in presence of $TmCl_3$ (0.1 wt%/styrene) and AA (2.0 wt%/styrene).

individual beads gives quantitative information about the metal ion content of the bead population. In Fig. 2, the population distribution is presented for the ^{169}Tm ion signal collected for 3 min (*ca.* 4×10^5 beads) for AA070-Tm. The *x*-axis of this plot is the intensity analog output of the TOF detector and is considered here as a relative number. The mean ^{169}Tm intensity is 81700.

The average number of metal ions per bead can be calculated from the mean intensity values as follow

$$N = \frac{I \times I_F}{T} \quad (2)$$

where I is the mean intensity measured by the TOF detector; I_F is the analog-to-count conversion factor for a particular ion (related to the mass response); and T is the transmission coefficient of the entire instrument. The transmission coefficient (the number of ions that reach the detector per number of ions injected) depends on tuning and the mass response of the instrument.

For the case of AA070-Tm, the value of I_F was 0.040 for (^{169}Tm) and T was 3.9×10^{-5}. The average Tm content of AA070-Tm was calculated to be 0.8×10^8 ^{169}Tm ions per bead. This level of loading is close to the saturation (upper limit) of the detector as manifested by the sharp drop in the Tm integrated intensity distribution (the right side of the distribution in Fig. 2). The width of the Tm intensity histogram showed $CV_{Tm} > 25\%$. These results are similar to the ones we obtained previously for Eu-containing beads.[22] In fact, detector saturation in the case of sample AA070-Tm indicates that the ^{169}Tm measured intensity and CV_{Tm} values are in error and likely to be different from the actual values. We conclude that lanthanide-containing polymer beads, synthesized at this high level of Ln ion content, do not meet the requirements for standard beads.

The next logical step was to decrease the amount of $TmCl_3$ salt added in the second stage of the 2-DisP. Sample AA086-Tm was prepared in the presence of 2.0 wt%/sty AA and 0.1 wt%/sty of $TmCl_3$, a factor of ten lower than that employed in the synthesis of sample AA070-Tm. The lanthanide-containing polymer beads produced were also monodisperse ($CV_d = 3.4\%$) with a size similar to that of AA070-Tm ($d = 1.9$ μm, see SEM images in Fig. S1, ESI‡). Fig. 3 shows the distribution of the integrated signal intensity for sample AA086-Tm. From the distribution average value, AA086-Tm beads were found to have *ca.* 1.1×10^7 ^{169}Tm atoms per bead. This number of atoms is adequate for mass cytometry measurements. However, CV_{Tm} was even higher (*ca.* 37%) than AA070-Tm and these values are too large for these beads to be used as mass cytometry standards. We know from our previous experiments[22] that the Ln content and Ln distribution values are independent of the type of Ln metal used in the 2-DisP bead synthesis. For example, very similar results were obtained when 0.1 wt%/sty of $TbCl_3$ was used instead of $TmCl_3$ (0.9×10^7 ^{159}Tb ions per bead and CV_{Tb} of *ca.* 41%). See Fig. S2, ESI,‡ for the mass cytometry measurement of AA083-Tb.

3-Stage dispersion polymerization

In Ref. 22, we showed that adding more acrylic acid plus a small amount of cross-linking agent to a dispersion polymerization reaction after more than half of the styrene was consumed led to particles with a narrower distribution of Ln ions per bead. We refer to this synthesis strategy as 3-stage dispersion polymerization (3-DisP). We used a similar protocol here in an attempt to synthesize beads suitable for mass cytometry calibration. The recipe is presented in Table 1, and the characteristics of sample AA120-Eu prepared in this way are listed as the third entry in Table 2. A scanning electron microscope image of these particles is presented in Fig. 4. The key result for this methodology is that the overall particle size is similar to that of sample AA070-Tm, and with a very narrow size distribution. Fig. 5 shows the mass cytometry distribution of AA120-Eu. Although the Eu atom content of AA120-Eu (calculated for ^{153}Eu from Fig. 5, *ca.* 1.1×10^7) is similar to Tm content of AA86-Tm, there is a substantial improvement in the bead-to-bead variation in lanthanide content per particle. For this sample, CV_{Eu} is 14%. This value is very similar to values for La and Tm found for sample AA105 whose

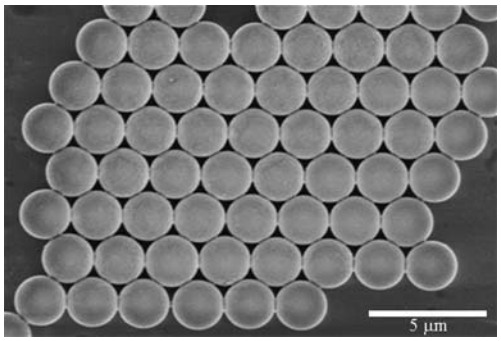

Fig. 4 SEM image of PS bead sample AA120-Eu synthesized by 3-DisP in the presence of 0.1% $EuCl_3$ added in the second stage with AA: 4 wt %/styrene ($d = 2.2$ μm, $CV_d = 1.6\%$).

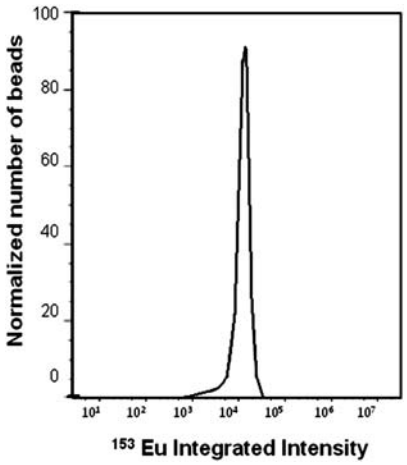

Fig. 5 Distribution of mass cytometry signal intensity for a population of PS beads (AA120-Eu) prepared by 3-DisP in presence of $EuCl_3$ (0.1 wt%/styrene) and AA (4.0 wt%/styrene). $CV_{Eu} = 14\%$.

synthesis was reported in Ref. 22. For the mass cytometry measurement of sample AA105, see Fig. S3, ESI.‡

To confirm the Eu-content of AA120-Eu obtained by mass cytometry, freeze-dried beads were microwave-digested in concentrated HNO_3 according to a reported protocol.[28] After digestion the solution were diluted and submitted for ICP-MS analysis. The results show that AA120-Eu sample has 7.6×10^6 (± 15%) ions per bead. This Eu-content value is about 25% less than was obtained by the mass cytometry (1.1×10^7 ions per bead); which means that the transmission factor T in eqn (2) is underestimated for the mass cytometry calculations. We are currently investigating this point to understand the reason behind this deviation.

Ion-release behaviour and mass cytometry calibration standard

Metal-containing beads synthesized by 3-DisP appear to retain their lanthanide content in aqueous solutions of different pH values, as explained in Ref. 22. That report described experiments carried out over a three-week time frame. For metal-containing beads to be suitable for mass cytometry instrument calibration, the metal content of the beads should be examined over longer storage times. Consequently, we decided to repeat

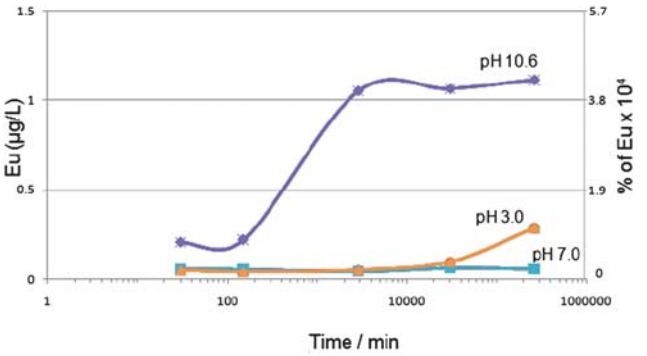

Fig. 6 ^{153}Eu ion release into the aqueous phase from colloidal suspensions of PS bead sample (0.5% solids content of AA120-Eu, synthesized by 3-stage DisP) in three different buffer solutions. Beads contain 260 μg L^{-1} Eu ion (w/w styrene). pH 10.6 buffer solution: 200 mM sodium carbonate/bicarbonate, pH 7.0 buffer solution: 10 mM ammonium acetate and pH 3.0 buffer solution: 50 mM sodium acetate. The right-hand y-axis represents the percentage of ^{153}Eu ion released into the aqueous phase to the number of ^{153}Eu-content of the beads.

the Ln ion-release study on sample AA120-Eu over a six-month period, which we believe is sufficient to judge their Ln-release behaviour.

We examined the stability of the beads in a range of aqueous media that are commonly utilized during cell analysis. We used conventional inductively coupled plasma-mass spectrometry solution analysis to follow the leakage of Ln ions (^{153}Eu in case of AA120-Eu) into the aqueous medium as a function of time. Experiments were performed on sample-Eu 120 synthesized by 3-DisP. This sample contains 260 ppm Eu ion (w/w based on polystyrene). The results presented in Fig. 6 are for 0.5 wt% beads in suspension in three aqueous solutions buffered at pH 3.0, 7.0 and 10.6. At pH 7, there is no measurable release of Eu^{3+} from the AA120-Eu beads over the entire period of study.

After 6 months at pH 3, sample AA120-Eu showed a minimal increase of the Eu^{3+} ions in the medium (*ca.* 0.3 μg L^{-1}). At pH 10.6, a small amount of Eu^3 ions was released into the continuous medium over the first two days to reach an Eu^{3+} concentration of 1.1 μg L^{-1}. This is about four times higher than that of pH 3, but corresponds to less than 0.01% of the Eu content of the beads. The release profile levelled off after two days, and no further loss of ions to the aqueous phase could be detected over the next six-months. Thus, we conclude that leakage of embedded Ln ions into the aqueous medium is unlikely to be a source of problems in using our lanthanide-containing beads for the calibration of the mass cytometry instrument.

Lanthanide-containing beads as internal standards for cell samples

Let us consider another way of presenting the mass cytometry results; through bivariate or scatter plots. The bivariate plots graph the relationship between two variables (isotopic concentrations) that have been measured on a single bead. Such a plot permits us to see at a glance the degree and pattern of the relation between the two isotopes in the sample. Most importantly, using bivariate plots, one can group the populations of the beads that have similar contents of different isotopes. On a bivariate plot,

the x- and y-axes can represent the concentration of any two isotopes of interest. Each point on the plot shows the x and y isotopic-content for a single bead.

Fig. 7 shows the two-dimensional projections (a bivariate plot)[32] of some multidimensional data sets obtained as a result of the mass cytometry experiment. Fig. 7A presents a logarithmic ^{151}Eu/^{153}Eu bivariate plot for the AA120-Eu sample. This is another way of presenting the same data used to construct Fig. 5. Although the beads show different intensities of Eu content ranging from *ca.* 10^3 up to 3×10^4 for both isotopes, the vast majority (> 90%) of the beads exhibit a very tight distribution of intensities around ca, 8×10^3. This behaviour in the bivariate plot of AA120-Eu sample reflects the characteristic feature of beads prepared by 3-Disp, which is their low bead-to-bead variability of the metal (Eu) content.

For comparison, we examined, by mass cytometry, the metal content of KG1a, a model human acute myelogenous leukemia cell line. These cells were fixed and then treated with an iridium intercalating agent that is taken up in amounts that reflect the DNA content of the cells. In Fig. 7B we present the ^{191}Ir/^{193}Ir bivariate plot for these cells. The broad area associated with the ^{191}Ir/^{193}Ir projection manifests the wide distribution of Ir-content of the KG1a cells. This type of result is expected from any cell line due to the variability of DNA content in a given cell.

The main goal for this work was to examine the usefulness of lanthanide-containing polymer beads as internal standards for cell line measurements by mass cytometry. Accordingly, we need to test the effect of mixing beads and cells on the mass cytometry response. In a proof of concept experiment, a sample of AA120-Eu beads was mixed with a suspension of KG1a cells. This cell line is well known to have a high level of CD34 antigen expression. Therefore, we separately stained its surface with CD34 monoclonal antibodies, which in turn were independently tagged with ^{169}Tm in the form of ions bound to a metal chelating polymer. [27] We denote these tagged antibodies uniformly as CD34-^{169}Tm because the observed difference in the staining efficiency is outside of scope of this paper. In addition, the KG1a cells were fixed and stained with the Ir-intercalator.[21]

Let us consider the ^{193}Ir/^{153}Eu bivariate projection for mass cytometry data obtained for a 100 : 1 mixture of KG1a cells and AA120-Eu beads as shown in Fig. 8. The cell-like events are Ir-positive and Eu-negative and appear in the upper left corner of the plot. The bead-only events are Eu-positive and Ir-negative and appear in the lower right corner of the plot in Fig. 8. In addition, there is a small population of events (*ca.* 2.2%) that show a Eu-positive and Ir-positive response in the upper right corner of the plot. This signal must correspond to beads and cells that interact or pass simultaneously through the plasma torch of the ICP mass spectrometer. This result is unexpected because the metal-containing PS beads are coated with a corona of polyvinylpyrrolidone that suppresses adsorption to the cells.[33]

To check if the CD34-^{169}Tm antibody was responsible for this interaction, we mixed AA120-Eu beads with a different cell line,

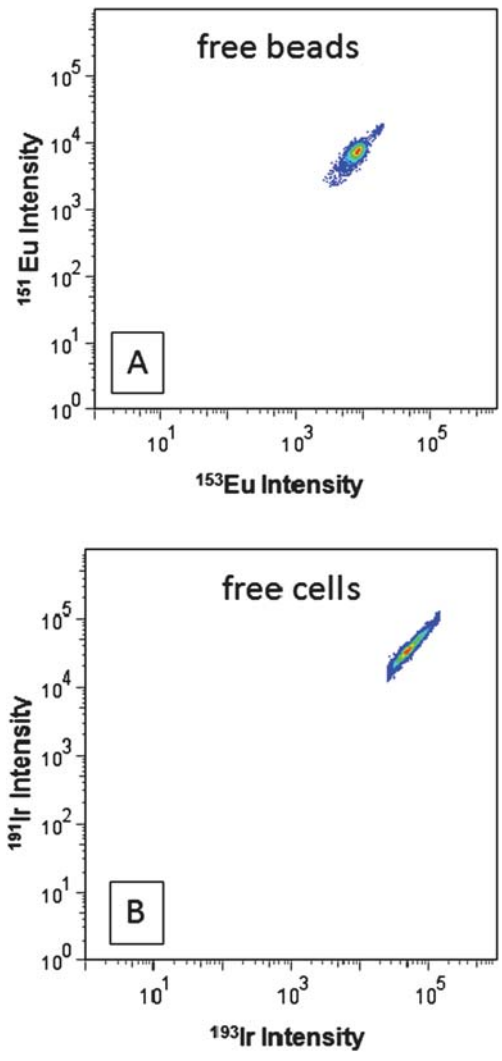

Fig. 7 Examples of bivariate plots of mass cytometric results for (A) free AA120-Eu beads and (B) KG1a free cells stained with CD34-^{169}Tm and Ir-interchelator.

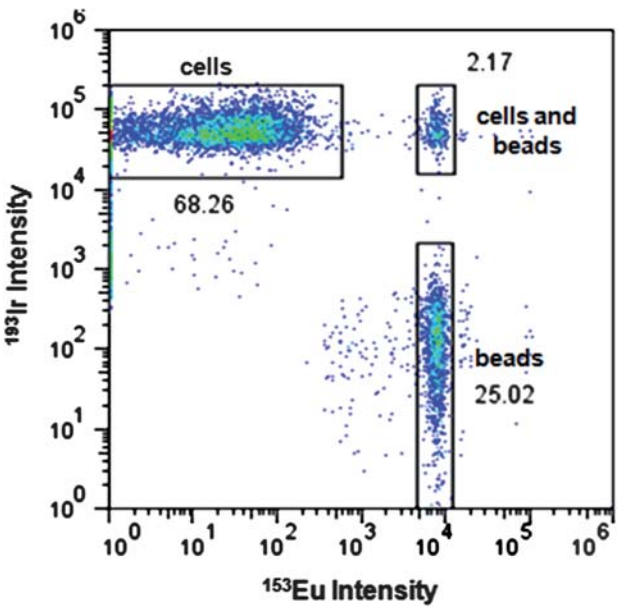

Fig. 8 A bivariate plot of mass cytometry results for: 100 : 1 mixture of cells and beads. Colored points represent the Ir- and Eu-positive events.

Table 3 Averages of the integrated ion intensities over the transient signals for individual KG1a, U937 cells, and AA120-Eu beads.[a]

Samples		Free Cells		Cells and beads			Free beads
		^{169}Tm	^{193}Ir	^{169}Tm	^{193}Ir	^{153}Eu	^{153}Eu
KG1a and AA120-Eu beads	K1	33 000	49 000	33 000	46 000	8000	7000
	K2	62 000	44 000	63 000	43 000	7000	7000
	K3	71 000	44 000	72 000	49 000	7000	7000
	K4	17 000	48 000	17 000	47 000	8000	7000
	K5	42 000	48 000	41 000	48 000	7000	7000
	K6	59 000	48 000	60 000	50 000	7000	7000
	K8	36 000	49 000	36 000	48 000	8000	7000
	K9	44 000	47 000	39 000	52 000	8000	7000
	K10	16 000	51 000	16 000	50 000	8000	7000
	K11	28 000	51 000	27 000	50 000	8000	7000
	K12	30 000	48 000	30 000	52 000	8000	8000
U937 and AA120-Eu beads	U1	160	51 000	166	51 000	10 000	9000
	U2	190	51 000	201	49 000	9000	9000
	U3	280	50 000	278	53 000	9000	9000
	U4	460	52 000	454	51 000	9000	9000
	U5	3300	51 000	3697	56 000	9000	9000
	U6	1900	55 000	434	50 000	9000	9000
	U7	530	50 000	772	50 000	9000	9000
	U8	590	50 000	531	50 000	10 000	9000
	U9	1700	50 000	1787	50 000	10 000	9000
	U10	390	51 000	411	54 000	9000	9000
	U11	280	53 000	324	53 000	9000	8000
	U12	460	52 000	771	46 000	9000	8000

[a] Sample replicates: K (KG1a) and U (U937) cells stained with ^{192}Ir intercalator and ^{169}Tm-labeled CD34. Each sample was examined in a 100 : 1 mixture with metal-containing beads AA120-Eu. The Eu content of the AA120-Eu gated without cells is reported in the last column.

U937 human leukemic monocyte lymphoma cells that have no CD34 antigen and were fixed and stained with CD34-^{169}Tm and Ir-intercalator. We observed very similar behaviour with the U937 cell line. This behaviour can be seen as a kind of "association" between the cells and metal-containing beads that occurred either during sample preparation or because of association as the samples entered the plasma torch. We do not yet have a clear explanation of this behaviour. Nevertheless, this interaction affects only a small fraction of the cells, and there is no significant difference between the metal-content of cells measured in the presence and absence of metal-containing beads, as can be estimated roughly by comparing the ^{193}Ir intensities in Fig. 7B and Fig. 8.

More mass cytometry results for 12 replicates of each KG1a (K1-K12) and U937 (U1-U12) cell lines mixed with AA120-Eu beads are presented in Table 3. In this table, each row represents one sample whose ^{169}Tm- and ^{193}Ir-contents were determined from two distributions. First, data for a cell population was gated on cells alone (free cells). Second, data were obtained for another population gated together with AA120-Eu beads (column head: cells and beads). The columns on the right-hand side of Table 3 represent the signal intensity associated with the ^{153}Eu-content of the AA120-Eu beads gated in the absence of cells. The data in Table 3 show that the ^{169}Tm- and ^{193}Ir-content of both KG1a and U937 cells were independent of the presence of the metal-containing beads.

Fig. 9 shows a plot of some of the mass cytometry data from Table 3. The *y*-axis presents signal intensities for ^{169}Tm- and ^{193}Ir for KG1a cell lines measured by mass cytometry in the presence of AA120-Eu beads. These values are plotted against the signal intensities for ^{169}Tm- and ^{193}Ir for KG1a (free cells) gated

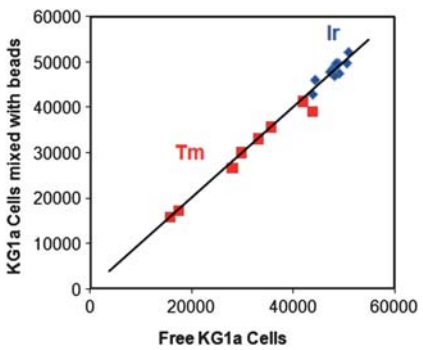

Fig. 9 Comparison between the ^{193}Ir (from DNA intercalator) and ^{169}Tm (from CD34-^{169}Tm) averages of integrated ion intensities over the transient signals for KG1a cells gated alone (*x*-axis) and in a mixture with AA120-Eu beads (*y*-axis).

excluding beads. The best-fit line drawn through the data has a slope of 1.0 and is passes through the origin. Accordingly, we conclude that the presence of the AA120-Eu beads does not affect the mass cytometry response to the metal content of the cells. Thus the metal-containing beads can be used as an internal standard in mass cytometry measurements on cell samples.

Conclusions

We report the synthesis of a series of metal-containing polystyrene beads with a very narrow size distribution, designed for the calibration of mass cytometry instruments. The PS bead samples reported here were synthesized by dispersion polymerization of styrene in ethanol. They contain up to 10^8 Ln ions per

bead but were optimized to contain about 10^7 Ln ions, a concentration that falls in the detection range of the mass cytometer and is suitable for beads to be employed as instrument standards. In general, the metal-containing beads synthesized by 2-stage dispersion polymerization in the presence of 0.1% $LnCl_3$ and 2% acrylic acid met the size, size distribution, and Ln-content requirements for the beads to be used as standard beads for mass cytometry measurements. A shortcoming of these beads was a large bead-to-bead variation in their lanthanide ion content. By modifying the particle synthesis strategy to add additional acrylic acid and a small amount of cross-linking reagent later in the reaction (3-stage dispersion polymerization, 3-DisP), a much lower bead-to-bead variation in the metal content was obtained.

Lanthanide-containing beads prepared by 3-DisP are stable when stored in buffer at pH values ranging from 3 to 10.6, with no significant leaching of their embedded Ln into aqueous media. When these beads were mixed with cell suspensions of two different cell lines (KG1a and U937), only about 2% of the total signal came from cells that associated with beads. There was no influence of the presence of the beads on the metal content of the cells determined by mass cytometry. We conclude that beads prepared by 3-DisP are well suited to be used as mass cytometry instrument calibration standards, and as internal standard beads for the measurement of the metal content of cells by mass cytometry.

Mass cytometry is a novel and rapidly improving analytical tool for phenotyping bioassays. We hope that the standard beads presented here will offer a way to obtain more consistent results and will help in improving the quality of the measurements using this technique.

Acknowledgements

The authors thank NSERC Canada, the National Institutes of Health [NIH grant R01-GM076127], Genome Canada, and the Ontario Genomics Institute for their support of this research.

References

1 N. Baumgarth and M. Roederer, *J. Immunol. Methods*, 2000, **243**, 77–97.
2 L. Belov, O. De la Vega, C. G. Dos Remedios, S. P. Mulligan and R. I. Christopherson, *Cancer Res.*, 2001, **61**, 4483–4489.
3 M. J. Borowitz, K. L. Guenther, K. E. Shults and G. T. Stelzer, *American Journal of Clinical Pathology*, 1993, **100**, 534–540.
4 M. Cazzola, *Haematologica*, 2009, **94**, 1041–1043.
5 P. K. Chattopadhyay, D. A. Price, T. F. Harper, M. R. Betts, J. Yu, E. Gostick, S. P. Perfetto, P. Goepfert, R. A. Koup, S. C. De Rosa, M. P. Bruchez and M. Roederer, *Nat. Med.*, 2006, **12**, 972–977.
6 W. M. Comans-Bitter, R. De Groot, R. Van den Beemd, H. J. Neijens, W. C. J. Hop, K. Groeneveld, H. Hooijkaas and J. J. M. Van Dongen, *J. Pediatr.*, 1997, **130**, 388–393.
7 G. Rothe and G. Schmitz, *Leukemia*, 1996, **10**, 877–895.
8 F. Truong, B. R. Smith, D. Stachurski, J. Cerny, L. J. Medeiros, B. A. Woda and S. A. Wang, *Leuk. Res.*, 2009, **33**, 1039–1046.
9 R. A. Hoffman, *Current protocols in cytometry/editorial board*, J. Paul Robinson, managing editor, 2005, Chapter 1.
10 L. Wang, A. K. Gaigalas, G. Marti, F. Abbasi and R. A. Hoffman, *Cytometry, Part A*, 2008, **73a**, 279–288.
11 A. Schwartz, E. Fernandez Repollet, R. Vogt and J. W. Gratama, *Cytometry*, 1996, **26**, 22–31.
12 R. F. Vogt Jr, W. E. Whitfield, L. O. Henderson and W. H. Hannon, *Methods*, 2000, **21**, 289–296.
13 Y. Wu, S. K. Campos, G. P. Lopez, M. A. Ozbun, L. A. Sklar and T. Buranda, *Anal. Biochem.*, 2007, **364**, 180–192.
14 S. Hansen, R. Dahl and H. J. Hoffmann, *J. Immunol. Methods*, 2008, **338**, 58–62.
15 I. M. Jensen, J. S. Kristensen, M. Thomsen, J. Ellegaard and P. Hokland, *Analytical Cellular Pathology*, 1993, **5**, 213–223.
16 M. Han, X. Gao, J. Z. Su and S. Nie, *Nat. Biotechnol.*, 2001, **19**, 631–635.
17 V. I. Baranov, Z. A. Quinn, D. R. Bandura and S. D. Tanner, *J. Anal. At. Spectrom.*, 2002, **17**, 1148–1152.
18 Z. A. Quinn, V. I. Baranov, S. D. Tanner and J. L. Wrana, *J. Anal. At. Spectrom.*, 2002, **17**, 892–896.
19 O. Ornatsky, V. I. Baranov, D. R. Bandura, S. D. Tanner and J. Dick, *J. Immunol. Methods*, 2006, **308**, 68–76.
20 O. I. Ornatsky, R. Kinach, D. R. Bandura, X. Lou, S. D. Tanner, V. I. Baranov, M. Nitz and M. A. Winnik, *J. Anal. At. Spectrom.*, 2008, **23**, 463–469.
21 O. I. Ornatsky, X. Lou, M. Nitz, S. Schafer, W. S. Sheldrick, V. I. Baranov, D. R. Bandura and S. D. Tanner, *Anal. Chem.*, 2008, **80**, 2539–2547.
22 A. I. Abdelrahman, S. Dai, S. C. Thickett, O. Ornatsky, D. Bandura, V. Baranov and M. A. Winnik, *J. Am. Chem. Soc.*, 2009, In Press.
23 D. R. Bandura, V. I. Baranov, O. I. Ornatsky, A. Antonov, R. Kinach, X. Lou, S. Pavlov, S. Vorobiev, J. E. Dick and S. D. Tanner, *Anal. Chem.*, 2009, **81**, 6813–6822.
24 S. D. Tanner, D. R. Bandura, O. Ornatsky, V. I. Baranov, M. Nitz and M. A. Winnik, *Pure Appl. Chem.*, 2008, **80**, 2627–2641.
25 S. D. Tanner, O. Ornatsky, D. R. Bandura and V. I. Baranov, *Spectrochim. Acta, Part B*, 2007, **62**, 188–195.
26 Stuart C. Thickett, Ahmed I. Abdelrahman, Olga Ornatsky, Dmitry Bandura, Vladimir Baranov and M. A. Winnik, *J. Anal. At. Spectrom.*, DOI: 10.1039/b916850h.
27 X. Lou, G. Zhang, I. Herrera, R. Kinach, O. Ornatsky, V. Baranov, M. Nitz and M. A. Winnik, *Angew. Chem., Int. Ed.*, 2007, **46**, 6111–6114.
28 L. Perring, M. I. Alonso, D. Andrey, B. Bourqui and P. Zbinden, *Anal. Bioanal. Chem.*, 2001, **370**, 76–81.
29 C. Vancaeyzeele, O. Ornatsky, V. Baranov, L. Shen, A. Abdelrahman and M. A. Winnik, *J. Am. Chem. Soc.*, 2007, **129**, 13653–13660.
30 H. B. Kagan, *Chem. Rev.*, 2002, **102**, 1805–1806.
31 J. S. Song, F. Tronc and M. A. Winnik, *J. Am. Chem. Soc.*, 2004, **126**, 6562–6563.
32 D. R. Parks, M. Roederer and W. A. Moore, *Cytometry, Part A*, 2006, **69a**, 541–551.
33 D. Wu, B. Zhao, Z. Dai, J. Qin and B. Lin, *Lab Chip*, 2006, **6**, 942–947.

